SCIENCE CHINA
Information Sciences

• RESEARCH PAPER •

December 2021, Vol. 64 222203:1–222203:14
https://doi.org/10.1007/s11432-020-3110-x

Optimal design of a scaled-up PRO system using swarm intelligence approach

Yingxue CHEN[1*], Zhongke SHI[2], Bin XU[2] & Mohammad Hasan SHAHEED[3]

[1]*School of Power and Energy, Northwestern Ploytechnical University, Xi'an* 710129*, China;*
[2]*School of Automatic, Northwestern Polytechnical University, Xi'an* 710129*, China;*
[3]*School of Engineering and Materials Science, Queen Mary University of London, London* E1 4NS*, UK*

Received 29 May 2020/Revised 14 August 2020/Accepted 1 October 2020/Published online 26 November 2021

Abstract In this study, the pressure-retarded osmosis (PRO) process is optimized using Harris hawks optimization (HHO)-based maximum power point tracking (MPPT) technology. To make the practical implementation of salinity-gradient-based energy harvesting using PRO feasible, MPPT is envisaged to play a substantial role. Therefore, this study focuses on the development of a novel MPPT controller using swarm intelligence. The HHO algorithm is the latest approach that mimics the unique chasing strategy of Harris hawks in nature. To test the cost effectiveness of the proposed method, two case studies with various operational scenarios are presented. Compared with the performance of selected well-known and recent approaches, such as perturb & observe, incremental mass resistance, and whale optimization algorithm techniques, that of the proposed metaheuristic-based MPPT technique is found to be highly competitive. Results also show that the proposed algorithm can overcome other methods' limitations, such as low tracking efficiency; low robustness when encountered in various operational conditions, including temperature and salinity; and steady-state oscillations. Furthermore, the proposed MPPT strategy is suitable for use in other fields of renewable energy harvesting.

Keywords maximum power point tracking (MPPT), swarm intelligence, metaheuristic algorithms, pressure-retarded osmosis (PRO), Harris hawks optimization (HHO)

Citation Chen Y X, Shi Z K, Xu B, et al. Optimal design of a scaled-up PRO system using swarm intelligence approach. Sci China Inf Sci, 2021, 64(12): 222203, https://doi.org/10.1007/s11432-020-3110-x

1 Introduction

To diminish global carbon emissions and establish renewable energy resources, new environmentally friendly sources of energy must be explored. Osmotic power generation from salinity gradient resources that use pressure retarded osmosis (PRO) has emerged as a potential source of renewable energy. In contrast to solar and wind energy, PRO can continuously operate day and night. Salinity gradient energy harvesting using PRO was first proposed by Loeb et al. [1, 2] in 1975. In the PRO process, low-concentration river water (i.e., feed solution) is driven by the osmotic pressure difference to penetrate a semipermeable membrane toward concentrated seawater (i.e., draw solution). When the hydraulic pressure is pressurized less than the osmotic pressure difference between the draw and feed solutions, the water flux is "retarded" through the membrane, generating extractable energy through a hydro turbine. A substantial amount of energy can be harvested from the spontaneous mixture of two different salinity solutions, namely, the draw and feed solutions. The potential of salinity gradient-based energy is enormous. Research shows that power can be theoretically obtained with the unit of TW globally when sea water and river water mix; then, 0.8 kilowatts of energy, which is equivalent to the energy extracted from a 280-m waterfall, can be harnessed per cubic meter [3, 4].

The most widely investigated controller in this context is the maximum power point tracking (MPPT) controller, which aims to track the maximum power point (MPP) under varying operational conditions. MPPT has become a research issue of renewable energy system fields with many magnificent applications.

* Corresponding author (email: yx.chen@nwpu.edu.cn)

To achieve highly efficient energy conversion concerning fluctuating environmental conditions in the real world, various MPPT-based methods have been devoted to the PRO system [5–9]. In the literature, two major MPPT algorithms (i.e., conventional and metaheuristic-based methods) are used for PRO modules. Traditional methods, such as perturb & observe (P&O) [10] and a variant of the incremental conductance method (IMR) [11], are inspired by classical MPPT methods in a PV system [12, 13]. However, the P&O and IMR algorithms must achieve a balance between the oscillations and the response speed, thus causing further power loss. Therefore, a robust and efficient MPPT method is required for a scaled-up PRO system. Furthermore, the authors in [5, 6] only optimized the hydraulic pressure with these two classic algorithms and variants of fuzzy logic control in a scaled-up PRO system to enhance the energy extraction process, which requires balance between the oscillations and the convergence speed. Even in the latest literature [8, 9], only conventional MPPT algorithms were applied for a PRO system. However, these traditional optimization methods are neither accurate nor efficient in complex optimization system design problems [14]. Some recent research has appropriately emphasized the importance and potential of metaheuristic algorithms in solving the MPPT problem of PRO systems [7, 15].

In consideration of these nonlinear global optimization difficulties and real-world problems, increased attention has been paid to swarm intelligence approaches [16–21]. The MPPT design combined with metaheuristic optimization algorithms is becoming popular progressively owing to its unique merit among current MPPT strategies, which are investigated by a few researchers as a low-cost and fast control technique. In PV systems, for example, the superiority of metaheuristic-based MPPT algorithms over other popular approaches is validated with promising results and a dramatically improved global optimization performance [22, 23]. Harris hawks optimization (HHO) was recently developed in 2019 by Heidari et al. [24], who were inspired by the chasing and cooperative activities of Harris hawks in nature. The experimental and comparative results demonstrate the excellent efficacy of HHO in the presence of an unknown environment, resulting in superior performance over other typical metaheuristic techniques [24]. The HHO algorithm has been reported to be utilized in several engineering design problems, and its prominent advantages in solving complicated optimization problems among swarm intelligence algorithms have also been validated [25, 26]. Thus, efficient MPPT technologies for a PRO plant have recently been developed and utilized to locate the MPP and improve efficiency. However, to the best of authors' knowledge, research on the metaheuristic-based MPPT approach for a PRO system is limited, and HHO is used for the first time for MPPT in this work [7].

In consideration of no-free-lunch theory, having only one specific optimal algorithm to explore the best solution for all optimization issues is impractical; hence, seeking adaption is an open problem [27, 28]. The favorable performance of an optimizer in a group of problems cannot assure equal performance on other kinds of issues [29]; this limitation is the foundation of this work. The HHO method is validated to solve complex problems in the real world [26, 30]; however, only a few HHO-based MPPT designs, especially for the PRO system, have been studied in the literature. Thus, an attempt is made to design a novel MPPT controller using an advanced HHO approach for a scaled-up PRO plant.

The novelty of this investigation is the design of an MPPT controller combined with the optimal swarm intelligence strategy for a PRO plant rather than using conventional MPPT methods. Therefore, the objective is to track the MPP with efficiency and robustness as operating condition varies. Section 2 of this paper presents the mathematical modeling of a PRO system, as well as its characteristics. Section 3 introduces the navigation and hunting hierarchy principle of the metaheuristic HHO algorithm. Section 4 outlines the general MPPT design based on the HHO strategy for a PRO plant. The simulation results and discussion with respect to various operational situations, including the concentration and flow rate of the feed solution, and temperature condition are presented in Section 5 to confirm the feasibility of the method. Lastly, Section 6 concludes the work.

2 Scaled-up PRO model

The overall operation of a PRO power plant with an MPPT controller is shown in Figure 1.

The MPPT controller measures the power feedback at each time interval. The control variable is the transit pressure from the high-pressure pump. As shown in Figure 1, the energy losses in the high-pressure pump (HP), energy recovery device (ERD), and hydro-turbine (HT) are considered. Most commercially available energy recovery devices consist of a turbocharger, Pelton wheel, and pressure exchanger. The efficiency of the pressure exchanger can be over 95% [31]. In applications, the energy losses mainly consist

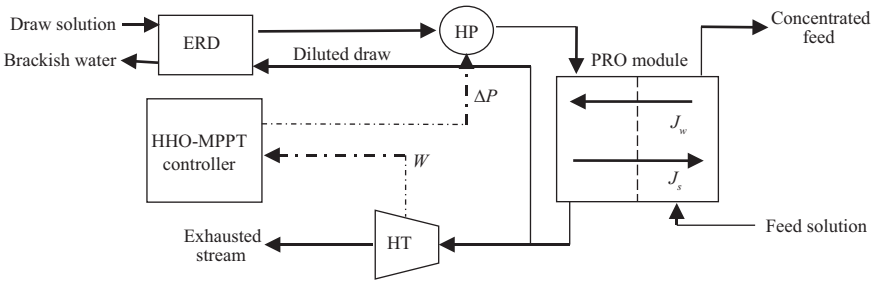

Figure 1 Schematic diagram of the PRO power plant.

of two parts: energy loss during the pressurizing process in the energy recovery device and high-pressure pump and that during the energy-generating process in the hydroturbine [32]. Thus, the efficiencies of the ERD, HP, and HT are considered in this work.

2.1 Pressure retarded osmosis power plant

The proposed controller is evaluated and utilized for a scaled-up PRO model incorporating detrimental effects (D-PRO) [30, 33]. In consideration of the influence of the detrimental effects, including external concentration polarization, internal concentration polarization, and reverse salt polarization, the water flux J_w and the reverse solute flux with experimentally measurable parameters are given by [34]

$$J_w = A_w \left(\left\{ \frac{\pi_D \exp(-\frac{J_w}{k}) - \pi_F \exp(J_w S/D)}{1 + B/J_w[\exp(J_w S/D) - \exp(-\frac{J_w}{k})]} \right\} - \Delta P \right), \tag{1}$$

$$J_s = B \left(\left\{ \frac{c_D \exp(-\frac{J_w}{k}) - c_F \exp(-J_w S/D_s)}{1 + \frac{B}{Jw}(\exp(-\frac{J_w S}{D}) - \exp(-\frac{J_w}{k}))} \right\} \right), \tag{2}$$

where A_w denotes the water permeability parameter, B denotes the salt permeability, D denotes the bulk diffusion coefficient, S denotes the structural coefficient of the membrane layer, k denotes the mass transfer coefficient of the draw boundary layer, and ΔP is the applied hydraulic pressure.

Solving the equations for the mass transfer of permeated water per unit membrane area yields the calculations for the volumetric flow rate of the permeating solution ΔV_p and reverse solution ΔV_s [35].

$$\mathrm{d}\left(\Delta V_p\right) = J_w \mathrm{d}\left(A_m\right), \tag{3}$$

$$\mathrm{d}\left(\Delta V_s\right) = J_s \mathrm{d}\left(A_m\right), \tag{4}$$

where A_m is the membrane area. The mass rate of the permeating solution Δq_p and reverse solution Δq_s are thus defined as [36]

$$\mathrm{d}\left(\Delta q_p\right) = \rho_P J_w \mathrm{d}\left(A_m\right), \tag{5}$$

$$\mathrm{d}\left(\Delta q_s\right) = \rho_D J_s \mathrm{d}\left(A_m\right), \tag{6}$$

where ρ_P is the permeating solution density, and ρ_D is the density of the draw solution. Specific energy extraction E is calculated by [35]

$$E = \frac{\Delta P \Delta V_P}{V_F^0}, \tag{7}$$

where V_F^0 denotes the initial feed flow rate. The average power density (APD) $\overline{\mathrm{PD}}$ is expressed as the specific energy per unit area to measure how fast the energy is generated. In this work, $\overline{\mathrm{PD}}$ is used to investigate the efficiency of various MPPT controllers [36],

$$\overline{\mathrm{PD}} = \frac{E}{A_m}. \tag{8}$$

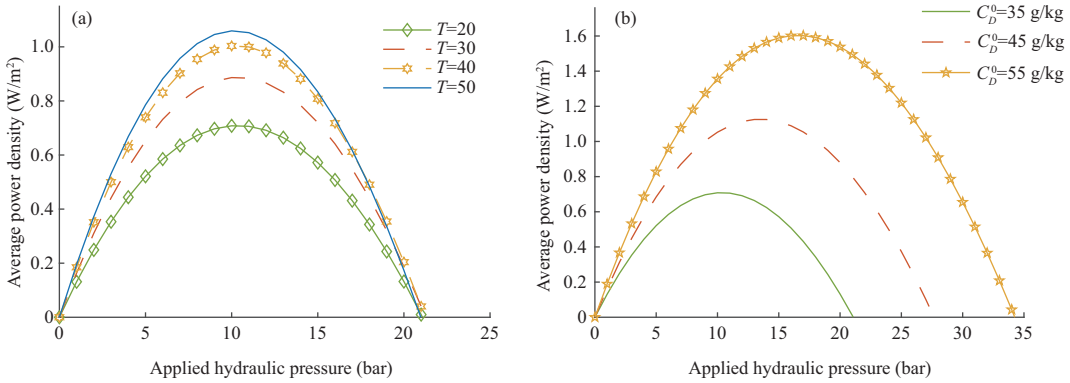

Figure 2 (Color online) $\overline{\mathrm{PD}} - \Delta P$ characteristics with respect to different temperatures (a) and salinity concentrations (b).

2.2 Characteristics of the PRO power plant

On the basis of the above mathematical model, the highly nonlinear properties of a scaled-up PRO power plant can be obtained. The characteristics are influenced by various factors, including membrane performance, component efficiencies, and operation conditions. In this subsection, three influential factors, including operating temperature and solution concentrations on the draw side, are evaluated by simulation. In Figure 2(a), the power-pressure ($\overline{\mathrm{PD}} - \Delta P$) characteristics subject to varying operating temperature T are shown. In Figure 2(b), the PRO characteristic curves regarding the fluctuations of draw concentration are illustrated. The MPP can be tracked from the PRO model under different operational conditions.

3 Harris hawks optimization method

HHO is a swarm intelligence method proposed in 2019 [24]; it mimics the cooperative foraging and hunting mechanism of Harris hawks in nature. The main strategy of these intelligent hawks is the "surprise pounce", namely, "seven skills". Dynamic situations call for various chasing styles, e.g., the escape patterns of a detected rabbit. The hawks are considered the smartest birds in nature; they can cooperate perfectly during the foraging process as a team [37,38]. When the leader gets lost while chasing the detected prey, switching mode occurs, and the other hawks take over the work. In this manner, the team becomes effective in finding and catching the target rabbit.

In the mathematical HHO model, the prey is considered the optimum. The above hunting strategy is simulated as the optimization process. When the hunting mechanism is introduced in designing the HHO method, three main mechanisms of hawks are considered: exploring prey, surprise pounce, and attacking the prey.

3.1 Exploring mechanism

In the exploring model, the Harris hawks track and detect the prey during the perching process. They are assigned to two groups randomly based on the random parameter q in (0,1). If $q < 0.5$, then the hawk roosts regarding the location of the team and the rabbit. If $q > 0.5$, then the hawk roosts randomly. The mathematical model of the updating position $X(k+1)$ in the next iteration t is mathematically expressed as [37]

$$X(t+1) = \begin{cases} X_{\mathrm{rand}}\,(t) - r_1\,|X_{\mathrm{rand}}\,(t) - 2r_2X(t)|\,, & q \geqslant 0.5, \\ (X_{\mathrm{rabbit}}\,(t) - X_m(t)) - r_1\,(\mathrm{LB} + r_2(\mathrm{UB} - \mathrm{LB}))\,, & q < 0.5, \end{cases} \tag{9}$$

where $X_{\mathrm{rand}}\,(t)$ and $X_{\mathrm{rabbit}}\,(t)$ indicate the randomly selected location of the hawks' population and the position of the prey, respectively. r is a random value in (0, 1). LB is the lower bound of variables, whereas UB is the upper bound. The average position of the current hawks' population $X_m(t)$ is obtained as

$$X_m(t) = \frac{1}{N}\sum_{i=1}^{N} X_i(t), \tag{10}$$

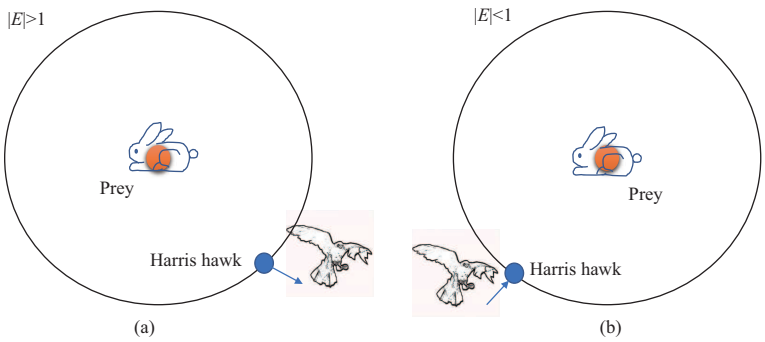

Figure 3 (Color online) Exploring (a) and exploitation (b) mode with respect to the value of E.

where $X_i(t)$ denotes the location of the hawk i, and N denotes the total number of hawks.

3.2 Transition mechanism

The exploitation modes are switched in consideration of the dynamic escaping prey energy. The energy is attained as [37]

$$E = 2 \times E_0 \left(1 - \frac{t}{T}\right), \tag{11}$$

where E_0 and E denote the initial and current escaping prey energy, respectively; t denotes the iteration number; E_0 is a random value in $(-1, 1)$ in each iteration t. According to (11), E is decreased from 2 to 0. If the value of E is greater than 1 or less than -1, then the current hawk is set to explore stochastically, as shown in Figure 3(a). Consequently, when the absolute value of the coefficient vector E is less than 1, the current search agent converges to the prey, as shown in Figure 3(b). The searching mode is an exploration phase, which is useful to avoid getting trapped in the local solutions.

3.3 Surprise pounce mechanism

The besiege process is the main optimization procedure here. The surprise pounce phase has four mechanisms based on the chasing activities of the Harris hawks, depending on the chance r of the successful escape of the prey and the retained prey energy E. In nature, hawks approach the intended prey slowly; when the prey loses energy, hawks start to besiege the exhausted prey. In the mathematical model, before the surprise pounce, if $r \geqslant 0.5$, then the prey fails to escape; if $r < 0.5$, then the prey escapes. When $|E| < 0.5$, the Harris hawk launches hard besiege; otherwise, a soft besiege is started.

3.3.1 *Soft besiege*

When $|E| \geqslant 0.5$, the rabbit has enough energy, the Harris hawks softly encircle and start the seven-skill process. If $r < 0.5$, then the prey escapes. In the real world, rabbits perform an escape pattern and leapfrog movements, and hawks dive rapidly and abruptly. In this regard, the levy flight (LF) function is introduced; this function mimics the real zigzag deceptive move of rabbits [24,38]. The LF-based motion is proven to be the optimal strategy; thus, this tactic is utilized in the mathematical model.

Hence, if $r < 0.5$ and $|E| \geqslant 0.5$, then choices X1 and X2 can possibly update the motion of the hawk:

$$X1 = X_{\text{rabbit}}(t) - E\,|JX_{\text{rabbit}}(t) - X(t)|\,, \tag{12}$$

$$X2 = X1 + S \times \text{LF}(D), \tag{13}$$

$$J = 2\,(1 - r_3)\,, \tag{14}$$

where J mimics the prey jumping ability in nature, D is the dimension of the problem. r_3 and S are random values in $(0, 1)$ and random vector of $1 \times D$ size, respectively. The levy flight conception LF is formulated as [39]

$$\text{LF}(x) = 0.01 \times \frac{r_4}{|r_5|^{\frac{1}{\beta}}} \left(\frac{\Gamma(1+\beta) \times \sin(\frac{\pi\beta}{2})}{\Gamma(\frac{1+\beta}{2}) \times \beta \times 2^{(\frac{\beta-1}{2})}}\right)^{\frac{1}{\beta}}, \tag{15}$$

where β is a constant equal to 1.5. The Harris hawk's final updated tactic is chosen in accordance with the following rules [24]:

$$X(t+1)=\begin{cases} X1, & \text{if fitness } (X1) < \text{ fitness } (X(t)),\\ X2, & \text{if fitness } (X2) < \text{ fitness } (X(t)). \end{cases} \tag{16}$$

If $r \geqslant 0.5$, then the prey fails to escape with enough energy, and the hawks start a soft besiege, gradually selecting the optimal dive toward the prey. In this regard, the tactic of the hawks is expressed as [24]

$$X(t+1)=\Delta X(t)-E\left|JX_{\text{rabbit}}(t)-X(t)\right|, \tag{17}$$

where $\Delta X(t)$ is the distance between the rabbit and the hawk and expressed as [24]

$$\Delta X(t)=X_{\text{rabbit}}(t)-X(t). \tag{18}$$

3.3.2 *Hard besiege*

Hard besiege occurs when $|E|<0.5$; the Harris hawks encircle hardly to perform the seven-skill procedure. If $r<0.5$, then the updating location of the Harris hawk in iteration t is similar to the soft besiege when the prey escapes. This time, the updated location is based on the average location $X_m(t)$ and the prey position, and it is expressed as [24]

$$X1=X_{\text{rabbit}}(t)-E\left|JX_{\text{rabbit}}(t)-X_m(t)\right|, \tag{19}$$

$$X2=X1+S\times \text{LF}(D), \tag{20}$$

$$X(t+1)=\begin{cases} X1, & \text{if } F(X1)<F(X(t)),\\ X2, & \text{if } F(X2)<F(X(t)). \end{cases} \tag{21}$$

Conversely, if $r \geqslant 0.5$, then the next position of the Harris hawk is calculated by [24]

$$X(t+1)=X_{\text{rabbit}}(t)-E|\Delta X(t)|. \tag{22}$$

The operators, such as the coefficient vector E and r, are utilized to assist in solving the MPPT problems, resulting in the local optima stagnation avoidance in the HHO-based MPPT algorithm. Furthermore, it can be implemented for the multipeak control systems. Moreover, for each Harris hawk, all the random parameters in $(0,1)$ are independent.

4 Overview of the proposed HHO-based MPPT method

The proposed HHO-based MPPT method is investigated specifically for a scaled-up PRO osmotic power plant in this section. Varying operating environments, such as temperature, salinity concentrations, and flow rates, yield different properties in a typical PRO system. The power generated from the PRO module comes from HT and is sensed by the HHO-based MPPT module. The controller is assumed to be able to sense parameters, including the instantaneous concentration and the flow rate values from the osmotic power plant. Then, the MPPT algorithm is executed to generate the pressure signals to the HP. The high-pressure pump works on the draw solution, and the pressure is assumed to be instantaneous values at this stage. In this work, the specific MPPT problem and the application of the HHO technique are depicted in Section 5.

4.1 Problem description

The optimization model considering constraints is developed as follows. The MPPT problem under varying situations is mathematically defined as

$$\begin{aligned} &\text{Consider:} && x=[x_1]=[\Delta p],\\ &\text{maximize:} && f(x)=\max(F(x))=\max(\overline{\text{PD}}(\Delta p)),\\ &\text{subject to:} && \Delta p \geqslant \text{lower boundary},\\ & && \Delta p < \text{higher boundary}. \end{aligned}$$

The most popular method to solve the MPPT problem in the PRO application is the P&O method [6]; Also, the IMR algorithm is proposed and inspired by the INC controller for the MPPT problem in a PV system [5].

In this work, a novel MPPT technique using an advanced control strategy is proposed on the basis of the chasing mechanism and social behavior of Harris hawks. $F(x)$ is considered to be the instantaneous power density at transient pump pressure x at the early stage; this assumption is similar to that of the previous studies [5–7]. The comparative results are provided in Section 5.

4.2 Overall execution of the HHO application

In the exploration mode, the hawk i perches on the tree. To formulate this exploration process mathematically, the solution of the current searching agent i is expressed as [24]

$$\left(\Delta P_i\right)_m(k) = \frac{1}{N}\sum_{i=1}^{N}\Delta P_i(k), \tag{23}$$

$$\Delta P_i(k+1) = \begin{cases} \left(\Delta P_i\right)_{\text{rand}}(k) - r_1\left|\left(\Delta P_i\right)_{\text{rand}}(k) - 2r_2\Delta P_i(k)\right|, & q \geqslant 0.5, \\ \left(\left(\Delta P_i\right)_{\text{best}}(k) - \left(\Delta P_i\right)_m(k)\right) - r_3\left(\text{LB} + r_4(\text{UB} - \text{LB})\right), & q < 0.5, \end{cases} \tag{24}$$

where q is a random value in $(0, 1)$, and $X_m(t)$ denotes the average solution of the search agents in iteration t.

At the soft besiege stage when the rabbit has enough energy, the hawk i chases the best solution with progressive and rapid dives if the rabbit escapes; this situation is modeled using an LF-based strategy as in [24]. The comparison between $\overline{\text{PD}}(X1)$ and $\overline{\text{PD}}(X2)$ is included in (27) in case that $X1$ and $X2$ perform well.

$$X1 = \left(\Delta P_i\right)_{\text{best}}(k) - E\left|J\left(\Delta P_i\right)_{\text{best}}(k) - \Delta P_i(k)\right|, \tag{25}$$

$$X2 = X1 + S \times \text{LF}(D), \tag{26}$$

$$\Delta P_i(k+1) = \begin{cases} X1, & \text{if } \overline{\text{PD}}(X1) > \overline{\text{PD}}\left(\Delta P_i(k)\right) \text{ and } \overline{\text{PD}}(X1) > \overline{\text{PD}}(X2), \\ X2, & \text{if } \overline{\text{PD}}(X2) > \overline{\text{PD}}\left(\Delta P_i(k)\right) \text{ and } \overline{\text{PD}}(X2) > \overline{\text{PD}}(X1). \end{cases} \tag{27}$$

Similarly, if the rabbit fails to escape, the hawks encircle the best solution softly, and the mathematic formulations are [24]

$$\Delta X(k) = \left(\Delta P_i\right)_{\text{best}}(k) - \Delta P_i(k), \tag{28}$$

$$\Delta P_i(k+1) = \Delta X(k) - E\left|J\left(\Delta P_i\right)_{\text{best}}(k) - \Delta P_i(k)\right|. \tag{29}$$

In the hard besiege behavior, the search agents hardly perform the surprise pounce. If the rabbit escapes successfully, then the search agent i intensifies the besiege process referring to LF-based motion with the following equations:

$$X1 = \left(\Delta P_i\right)_{\text{best}}(k) - E\left|J\left(\Delta P_i\right)_{\text{best}}(k) - \left(\Delta P_i\right)_m(k)\right|, \tag{30}$$

$$X2 = X1 + S \times \text{LF}(D), \tag{31}$$

$$\Delta P_i(k+1) = \begin{cases} X1, & \text{if } \overline{\text{PD}}(X1) > \overline{\text{PD}}\left(\Delta P_i(k)\right), \\ X2, & \text{if } \overline{\text{PD}}(X2) > \overline{\text{PD}}\left(\Delta P_i(k)\right), \end{cases} \tag{32}$$

where the fitness function is formulated as [24]

$$\overline{\text{PD}}\left(\Delta p_i\right)(k+1) > \overline{\text{PD}}\left(\Delta p_i\right)(k). \tag{33}$$

If the prey is exhausted, then the search agent i starts the surprise pounce. The mathematical model is calculated as [24]

$$\Delta P_i(k+1) = \left(\Delta P_i\right)_{\text{best}}(k) - E|\Delta X(k)|. \tag{34}$$

The flow chart of the implementation is represented in Figure 4. First, the HHO algorithm and the PRO model are initialized. Afterward the loop starts, the location of the current Harris hawk is updated

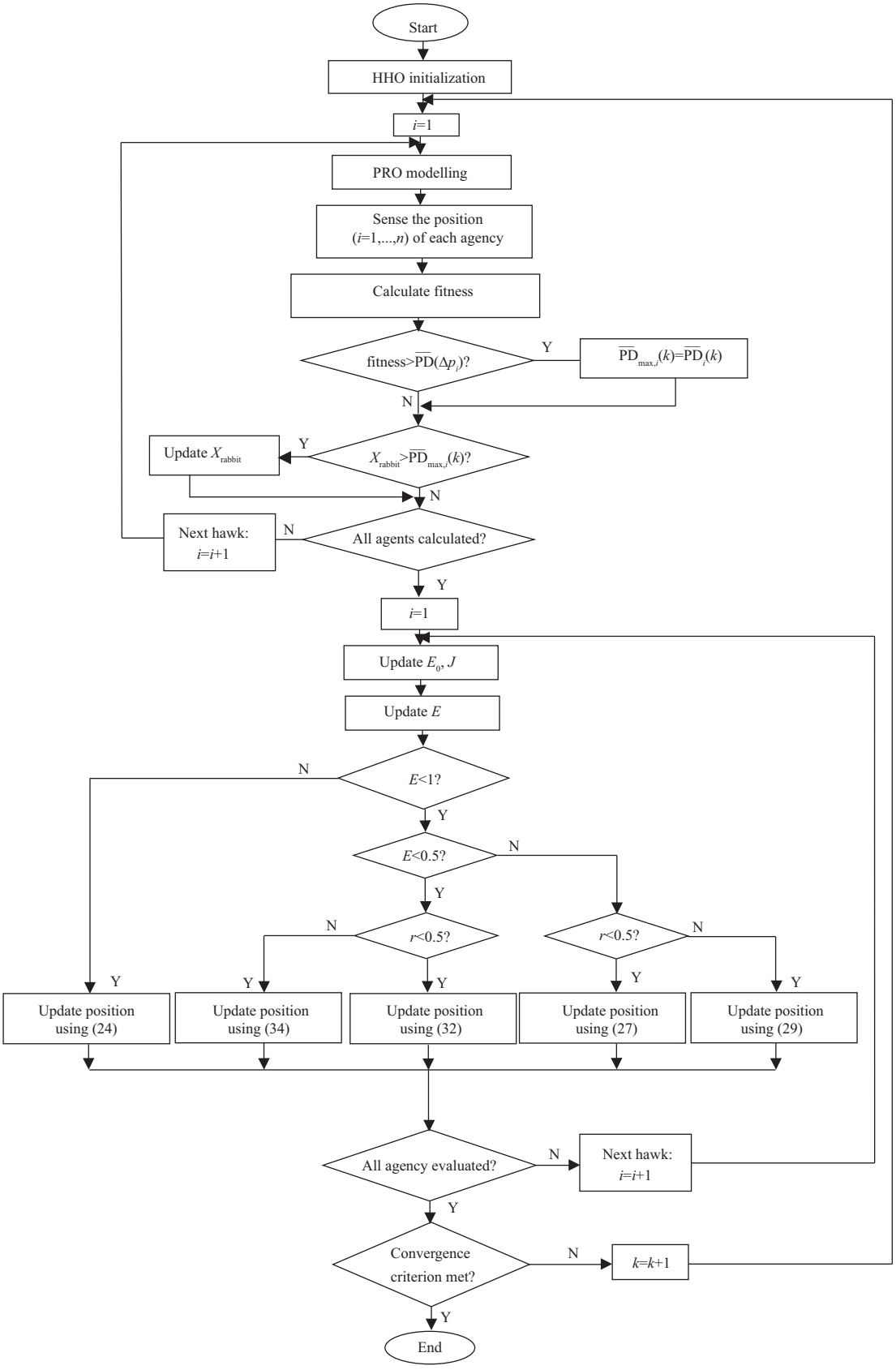

Figure 4 Overall procedure of the proposed HHO design for a PRO system.

in accordance with the HHO algorithm with respect to the cost function (33) at each iteration k. Then, its fitness is updated and compared with the other solutions. If the current fitness solution is larger than the fittest solution of rabbits, then the best fitness and the best location are replaced by that of the current search agent i. All search agents are used to find the global best solutions in the search space. Afterward, the rabbit location is updated at each iteration. Finally, the HHO parameter is updated with regard to HHO algorithm using (23)–(34). The probable prey position is estimated. The process is then repeated with respect to the potential prey location obtained from the previous iteration. At the end of the iterations, the solution obtained by the leader of the Harris hawks is considered as the optimum solution in the HHO-based MPPT design.

This HHO-based MPPT algorithm utilizes multiple Harris hawks to chase the prey position guided by the optimal Harris hawk. In other words, the hunting of every search agent considers their own fittest solution, as well as the best fitness from the group. E and r are generated stochastically; thus, they vary at each calculation. These random values, which are extracted over the course of iterations, favor avoiding the local optima. For each study, the HHO algorithm is applied under different situations. The statistical results extracted by the HHO-based MPPT controller are reported.

5 Results and discussion

The proposed MPPT design for the PRO system is designed to extract the maximum power under various operational conditions, including the temperature and the salinity profiles. The performance evaluation of the proposed HHO-based MPPT design is performed using a boost pump, which is illustrated in Section 2. To test the proposed method, the improvements of the MPPT performance are evaluated by simulations. Two case studies aiming at rapidly changing temperature and operational salinity conditions are then presented. In the first case, the performance is probed with the highly popular P&O and IMR methods to verify the superiority of the proposed technique [5,6]. In this MPPT problem, the controllers are designed to produce control signals and generate instantaneous variables to track the maximum value.

Two assumptions are held at the early stage. First, the pressure is adjusted by a stable and fast controller. Second, the instant sample period is larger than the pressure transition time at each step.

5.1 Case 1: rapidly changing temperature levels

The variations in temperature are considered in this subsection to evaluate the performance of the proposed method. In this case study, four various temperatures are set to increase from 20°C to 50°C, as shown in Figure 5.

The power under the changing temperature configuration utilizing P&O, IMR, and HHO is depicted in Figure 6. The results show a considerable improvement in tracking the MPP using the HHO algorithm. Furthermore, HHO methods provide a faster tracking speed under rapidly changing operational conditions compared with traditional MPPT approaches. In the dual stage PRO system, the osmotic power output increases [40].

Furthermore, the osmotic power values extracted from the PRO system with three techniques under consecutive step changes of operating temperature from 20°C to 50°C are illustrated in Table 1.

Table 1 shows the detailed data obtained from three MPPT methods. At the beginning with a temperature of 20°C, HHO can track the MPP of 0.70885380 W, P&O searches the MPP of 0.70803954 W, whereas IMR fails to locate the MPP and settle at 0.69696450 W. When the temperature is changed to 30°C, the MPPT methods are restarted to track the MPP, HHO can capture the MPP of 0.88741488 W, IMR finds the MPP of 0.88632589 W, and P&O fails to track the MPP at 0.88422936 W. All results are summarized in Table 1, which reveals that the conventional methods, i.e., P&O and IMR, cannot obtain the GMPP because these techniques must select the applied perturbation. In other words, they should make a trade-off between the oscillations and the convergence rate.

Among these algorithms, the HHO-MPPT controller is robust as an oscillation-free technique, resulting in fewer oscillations near the MPP and higher convergence speed. Moreover, the MPPT problem with the HHO controller can yield more osmotic power, resulting in a higher power efficiency under rapidly changing operational conditions.

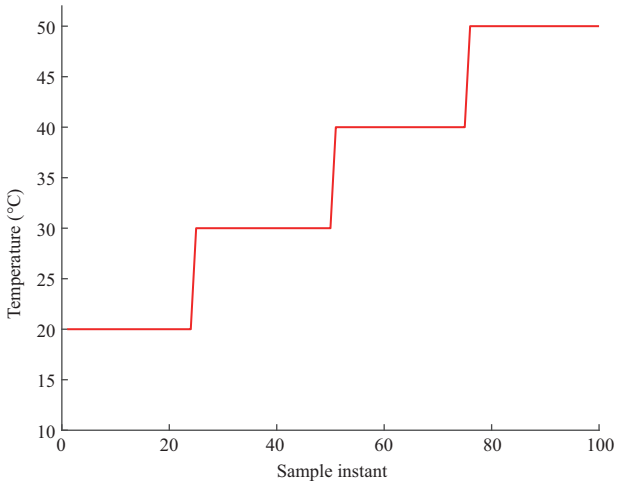

Figure 5 (Color online) Fluctuation configurations of four consecutive step changes of operating temperature from 20°C to 50°C.

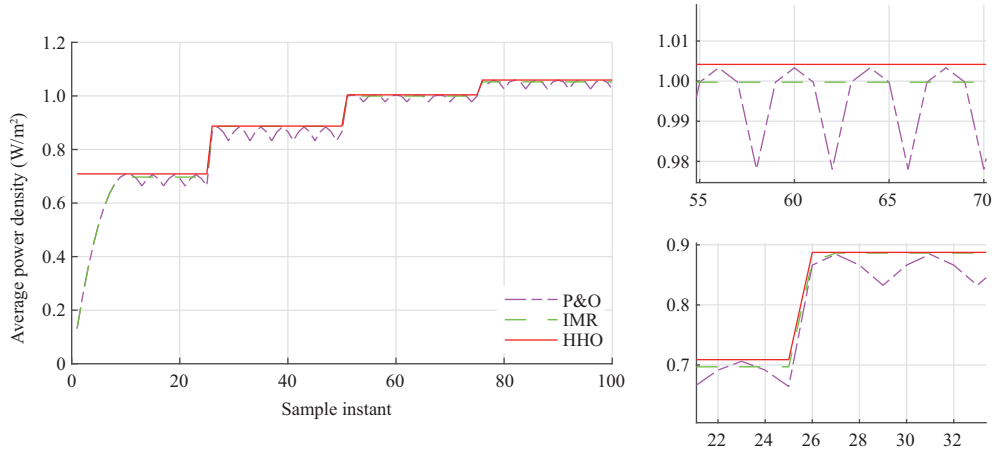

Figure 6 (Color online) APD results obtained in the PRO system using P&O, IMR and HHO algorithms under temperature variation.

Table 1 Optimal APD results under variations of temperatures obtained by three algorithms

Sample instant	Tracking techniques	Maximum power density (W/m^2)
0–25	P&O	0.70803954
	IMR	0.69696450
	HHO	0.70885380
26–50	P&O	0.88422936
	IMR	0.88632589
	HHO	0.88741488
51–75	P&O	1.00331396
	IMR	1.00331396
	HHO	1.00416676
76–100	P&O	1.05910919
	IMR	1.05242449
	HHO	1.05938094

5.2 Case 2: rapidly changing salinity levels

For further comparison of the effectiveness of the proposed HHO method, a complex operational condition is investigated, and the state-of-the-art metaheuristic method, whale optimization algorithm (WOA), is utilized. The variations in the salinity concentration and flow rate are considered, as shown in Figure 7.

The MPPT controller using HHO, P&O, IMR, and WOA techniques is implemented under these

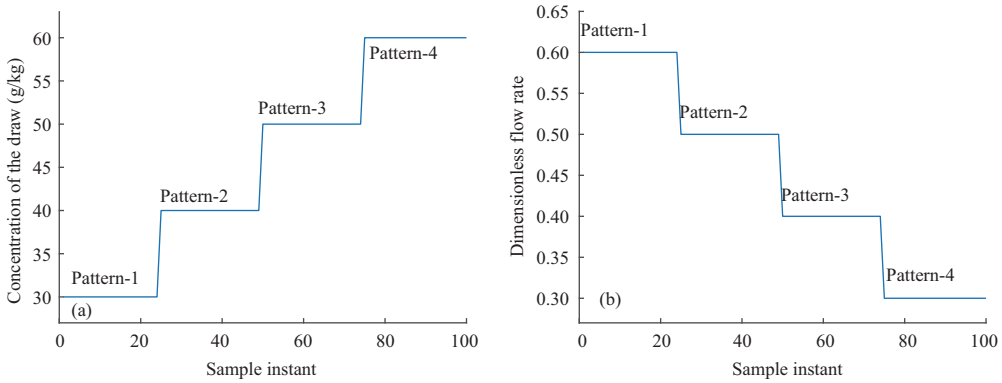

Figure 7 (Color online) Fluctuation configurations of (a) changing concentrations on the draw side and (b) varying dimensionless flow rates.

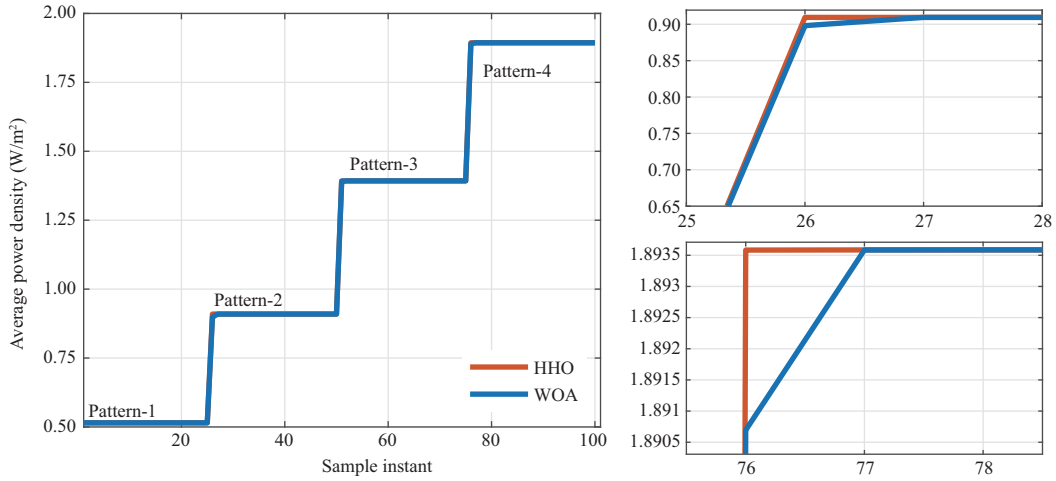

Figure 8 (Color online) APD results under varying operational conditions with four MPPT methods.

operational conditions. The result is presented in Figures 8 and 9. As shown in Figure 8, classical MPPT algorithms P&O and IMR show limited ability to find the maximum power efficiently under dynamic change conditions of concentration and flow rates. P&O takes 10 intervals at the beginning and four intervals for the salinity change from pattern-2 to pattern-3 to reach the MPP; in the case of IMR, the performance is improved for both situations, i.e., it takes nine and three intervals, respectively, to track the MPP. In this situation, the WOA and HHO perform significantly well and can capture the MPP in only one time instant (acceptable error: 0.001%), and HHO performs slightly better than WOA. For further comparison between these two established swarm intelligence methods, namely, WOA and HHO, the results are presented in Figure 9. Detailed data are listed in Table 2.

Table 2 shows the complete comparison of the response step. These results illustrate that the proposed metaheuristic algorithm can reach the MPP with the fastest speed in comparison with the four general techniques, favoring oscillation avoidance and less power loss. Again, the superior performance of the HHO technique-based MPPT method over all other methods is confirmed. In the beginning, the MPP extracted using HHO is 0.5149641572 W, where IMR reaches the MPP of 0.5137879625 W and the P&O algorithm settles at 0.5149391786 W. This result indicates that the tracking ability of the HHO is higher, resulting in higher power efficiency.

The simulation results reveal that the HHO-based MPPT design outperforms the P&O, IMR, and WOA techniques in terms of the reduction of steady-state oscillation, tracking speed, and tracking efficiency. Furthermore, the convergence time and the maximum power obtained by the four methods are briefly summarized in Table 2, with the purpose of quantitative comparison. The proposed technique outperforms other metaheuristic methods in terms of solving MPPT problems. The results reveal that the proposed HHO-based MPPT method can effectively and robustly handle the MPPT problem.

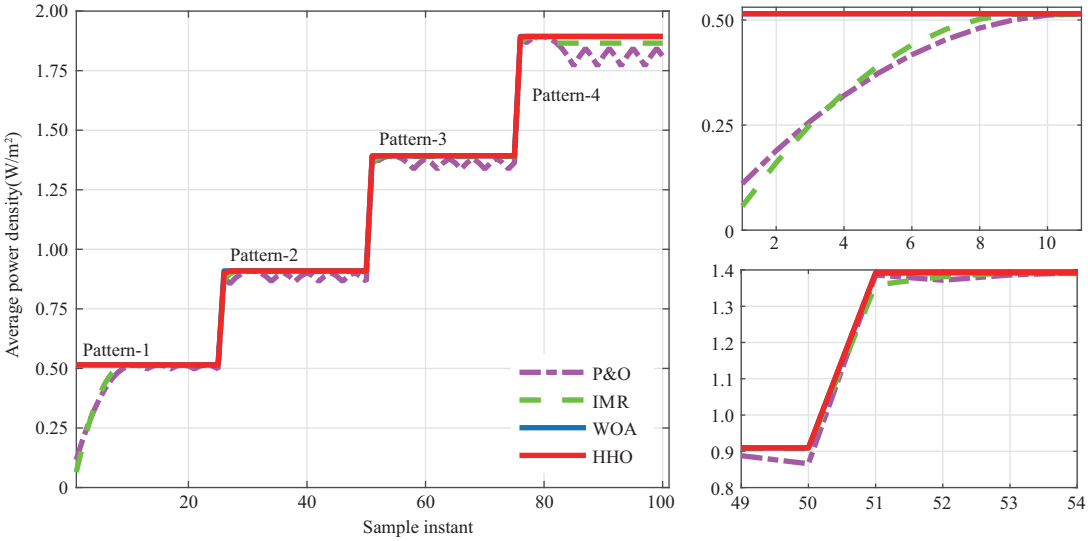

Figure 9 (Color online) Detailed APD results in the PRO system with HHO and WOA algorithms under changing operational conditions.

Table 2 Optimal APD results under variations of operating conditions obtained by four algorithms

Method	Convergence (W/m^2)				Tracking time (step)			
	Pattern-1	Pattern-2	Pattern-3	Pattern-4	Pattern-1	Pattern-2	Pattern-3	Pattern-4
P&O	0.5149391786	0.9090318523	1.3923453977	1.8926135716	10	4	2	4
IMR	0.5137879625	0.9083196469	1.3919964890	1.8935347161	9	3	3	3
WOA	0.5149641533	0.9094776519	1.3926700928	1.8935866382	2	2	2	2
HHO	0.5149641572	0.9094776554	1.3926701287	1.8935870002	1	1	1	1

6 Conclusion

The proposed HHO-based MPPT metaheuristic algorithm with 100 iterations and 70 search agents is evaluated on the MPPT problem and compared with existing MPPT methods. For the energy produced by the PRO process to be practical, its production cost must be comparable with other renewable energy sources (such as wind, hydro, and solar), thus requiring substantial development to improve the efficiency of the PRO process, mainly in terms of convergence speed and maximum extracted energy. By rapidly achieving the global optimum, small deviation and short tracking steps can lead to a superior MPPT performance. Similar to the MPPT methods of the PV system, traditional methods P&O and IMR have to balance the oscillation and tracking speed. In consideration of these indicators of the MPPT controller for an osmotic power plant, the robustness of the HHO-MPPT method around the MPP and low steady-state oscillations are verified by the results. Moreover, the results of the proposed method show superior convergence speed. The results also show a high MPP value obtained by HHO, resulting in less power loss and high power efficiency.

In summary, a fair comparison with some research is conducted in terms of tracking accuracy and convergence speed, leading to a favorable performance of the PRO plant with respect to an unknown operational condition. The superior performance of the proposed HHO-based algorithm in solving MPPT problems is proven to be efficient for a PRO-based salinity energy extraction system. The comprehensive study and simulation results validate that the proposed technique can substantially improve power efficiency. Furthermore, the proposed algorithm illustrates its ability to solve problems with challenging search spaces. The results also demonstrate that the proposed HHO method has superior performance in unconstrained and constrained problems. Lastly, the results of the design illustrate that the HHO-based MPPT algorithm has high performance in multipeak MPPT problems, also showing the applicability of the proposed MPPT method in solving real-world problems.

In future research, optimization studies of novel PRO configurations, such as dual-stage PRO and hybrid PV/RO/PRO systems, can be conducted to increase the overall potential extractable energy. In addition, the updated optimization algorithms and their variants can be combined in the above system

to improve the cost effectiveness and performance of the PRO process.

Acknowledgements This work was supported in part by National Natural Science Foundation of China (Grant Nos. 61933010, 61803305), Shaanxi Natural Science Foundation (Grant Nos. 2020JQ-223, 2019JZ-08, 2020JQ-213), and Aeronautical Science Foundation of China (Grant No. 201905053005).

References

1 Loeb S, Norman R S. Osmotic power plants. Science, 1975, 189: 654–655
2 Loeb S. Production of energy from concentrated brines by pressure-retarded osmosis. J Membrane Sci, 1976, 1: 49–63
3 Pattle R E. Production of electric power by mixing fresh and salt water in the hydroelectric pile. Nature, 1954, 174: 660
4 Logan B E, Elimelech M. Membrane-based processes for sustainable power generation using water. Nature, 2012, 488: 313–319
5 He W, Wang Y, Shaheed M H. Maximum power point tracking (MPPT) of a scale-up pressure retarded osmosis (PRO) osmotic power plant. Appl Energy, 2015, 158: 584–596
6 He W, Luo X, Kiselychnyk O, et al. Maximum power point tracking (MPPT) control of pressure retarded osmosis (PRO) salinity power plant: development and comparison of different techniques. Desalination, 2016, 389: 187–196
7 Chen Y, Vepa R, Shaheed M H. Enhanced and speedy energy extraction from a scaled-up pressure retarded osmosis process with a whale optimization based maximum power point tracking. Energy, 2018, 153: 618–627
8 Maisonneuve J, Chintalacheruvu S. Increasing osmotic power and energy with maximum power point tracking. Appl Energy, 2019, 238: 683–695
9 Long R, Lai X, Liu Z, et al. Pressure retarded osmosis: operating in a compromise between power density and energy efficiency. Energy, 2019, 172: 592–598
10 Wasynezuk O. Dynamic behavior of a class of photovoltaic power systems. IEEE Trans Power Apparatus Syst, 1983, PAS-102: 3031–3037
11 Hussein K H, Muta I, Hoshino T, et al. Maximum photovoltaic power tracking: an algorithm for rapidly changing atmospheric conditions. IEE Proc Gener Transm Distrib, 1995, 142: 59–64
12 Mousa H H H, Youssef A R, Mohamed E E M. Variable step size P&O MPPT algorithm for optimal power extraction of multi-phase PMSG based wind generation system. Int J Electrical Power Energy Syst, 2019, 108: 218–231
13 Kumar R, Khandelwal S, Upadhyay P, et al. Global maximum power point tracking using variable sampling time and p-v curve region shifting technique along with incremental conductance for partially shaded photovoltaic systems. Sol Energy, 2019, 189: 151–178
14 Dufo-López R, Bernal-Agustín J L, Contreras J. Optimization of control strategies for stand-alone renewable energy systems with hydrogen storage. Renew Energy, 2007, 32: 1102–1126
15 Chen Y, Alanezi A A, Zhou J, et al. Optimization of module pressure retarded osmosis membrane for maximum energy extraction. J Water Process Eng, 2019, 32: 100935
16 Liu Y, Zhang Y, Li P, et al. Uncalibrated downward-looking UAV visual compass based on clustered point features. Sci China Inf Sci, 2019, 62: 199202
17 Chen D, Li W, Liu X, et al. Effects of measurement noise on flocking dynamics of cucker-smale systems. IEEE Trans Circ Syst II, 2020, 67: 2064–2068
18 Duan H B, Zhang D F, Fan Y M, et al. From wolf pack intelligence to UAV swarm cooperative decision-making (in Chinese). Sci Sin Inform, 2019, 49: 112–118
19 Guo Y Y, Xu B, Han W X, et al. Robust adaptive control of hypersonic flight vehicle with asymmetric AOA constraint. Sci China Inf Sci, 2020, 63: 212203
20 Zhang R, Xu B, Wei Q, et al. Harmonic disturbance observer-based sliding mode control of MEMS gyroscopes. Sci China Inf Sci, 2022, 65: 139201
21 Chen D, Kang M, Yu W. Probabilistic causal inference for coordinated movement of pigeon flocks. EPL, 2020, 130: 28004
22 Yang B, Zhang X, Yu T, et al. Grouped grey wolf optimizer for maximum power point tracking of doubly-fed induction generator based wind turbine. Energy Convers Manage, 2017, 133: 427–443
23 Ann R A, Kalaivani L. A GOA-RNN controller for a stand-alone photovoltaic/wind energy hybrid-fed pumping system. Soft Comput, 2019, 23: 12255–12276
24 Heidari A A, Mirjalili S, Faris H, et al. Harris hawks optimization: algorithm and applications. Future Generation Comput Syst, 2019, 97: 849–872
25 Chen H, Jiao S, Wang M, et al. Parameters identification of photovoltaic cells and modules using diversification-enriched Harris hawks optimization with chaotic drifts. J Cleaner Production, 2020, 244: 118778
26 Houssein E H, Hosney M E, Oliva D, et al. A novel hybrid Harris hawks optimization and support vector machines for drug design and discovery. Comput Chem Eng, 2020, 133: 106656
27 Wolpert D H, Macready W G. No free lunch theorems for optimization. IEEE Trans Evol Computat, 1997, 1: 67–82
28 Wang L, Wang W, Wang Y Y, et al. Feasibility of reinforcement learning for UAV-based target searching in a simulated communication denied environment (in Chinese). Sci Sin Inform, 2020, 50: 375–395
29 Neggaz N, Houssein E H, Hussain K. An efficient Henry gas solubility optimization for feature selection. Expert Syst Appl,

2020, 152: 113364

30 Ridha H M, Heidari A A, Wang M, et al. Boosted mutation-based Harris hawks optimizer for parameters identification of single-diode solar cell models. Energy Convers Manage, 2020, 209: 112660

31 Avlonitis S A, Kouroumbas K, Vlachakis N. Energy consumption and membrane replacement cost for seawater RO desalination plants. Desalination, 2003, 157: 151–158

32 He W, Wang Y, Mujtaba I M, et al. An evaluation of membrane properties and process characteristics of a scaled-up pressure retarded osmosis (PRO) process. Desalination, 2016, 378: 1–13

33 Kim Y C, Elimelech M. Potential of osmotic power generation by pressure retarded osmosis using seawater as feed solution: analysis and experiments. J Membrane Sci, 2013, 429: 330–337

34 Yip N Y, Elimelech M. Thermodynamic and energy efficiency analysis of power generation from natural salinity gradients by pressure retarded osmosis. Environ Sci Technol, 2012, 46: 5230–5239

35 He W, Wang Y, Shaheed M H. Modelling of osmotic energy from natural salt gradients due to pressure retarded osmosis: effects of detrimental factors and flow schemes. J Membrane Sci, 2014, 471: 247–257

36 Straub A P, Lin S, Elimelech M. Module-scale analysis of pressure retarded osmosis: performance limitations and implications for full-scale operation. Environ Sci Technol, 2014, 48: 12435–12444

37 Lefebvre L, Whittle P, Lascaris E, et al. Feeding innovations and forebrain size in birds. Anim Behaviour, 1997, 53: 549–560

38 Bednarz J C. Cooperative hunting in Harris' hawks (Parabuteo unicinctus). Science, 1988, 239: 1525–1527

39 Yang X-S. Nature-Inspired Metaheuristic Algorithms. Frome: Luniver Press, 2010

40 He W, Wang Y, Shaheed M H. Enhanced energy generation and membrane performance by two-stage pressure retarded osmosis (PRO). Desalination, 2015, 359: 186–199